Robotica (2017) volume 35, pp. 2201–2217. © Cambridge University Press 2017
doi:10.1017/S0263574716000801

Observer-based two-time scale robust control of free-flying flexible-joint space manipulators with external disturbances

Xiaoyan Yu* and Li Chen

School of Mechanical Engineering and Automation, Fuzhou University, Fuzhou 350116, Fujian Province, China
E-mail: chnle@fzu.edu.cn

(Accepted October 31, 2016. First published online: March 21, 2017)

SUMMARY
Observer-based two-time scale robust control is proposed for free-flying flexible-joint space manipulators with unknown payload parameters and bounded disturbances. The dynamic equations of a free-flying space manipulator with two flexible revolute joints were derived by the momentum conservation law and the Lagrange equations. A flexibility compensator was introduced to make the equivalent joint stiffness large enough, which made traditional singular perturbation approach applicable. Then, a singular perturbation model was formulated and a reduced-order controller is proposed. This controller consisted of a slow sub-controller and a fast flexible-joint sub-controller. To the slow subsystem, a sliding observer based robust slow sub-controller was proposed. By optimal linear quadratic regulator method, the fast sub-controller was designed with the estimated velocity by linear observer. This fast sub-controller could stabilize the fast subsystem around the equilibrium trajectory created by the slow subsystem under the effect of the slow control. Finally the numerical simulations were carried out, which showed that elastic joint vibrations had been stabilized effectively and good tracking performances had been achieved.

KEYWORDS: Free-flying flexible-joint space manipulator, Two-time scale control, Singular perturbation theory, Robust control, State observer.

1. Introduction

Robots are playing important roles in outer space operation.[1–11] The environment in outer space is threatening, it is difficult and hazardous for human beings to work there. Orbiting robots can be used for servicing satellites. In this case, manipulators need to be used to chase the target satellite. Differing from the terrestrial systems, the base attitude and orbital dynamics are coupled, so its links' locomotion leads to the base's reactions, and consequently a variation of the end-effector position. To achieve a good tracking performance of space-based manipulators, various control algorithms have been developed. Since no perfect and exact dynamic model could be derived for all the space manipulators, adaptive control, robust control and adaptive robust control techniques have been proposed to control rigid space manipulator. Walker *et al.*[6] presented an adaptive control method that achieves globally stable trajectory tracking with uncertainties in the inertial parameters of the system. Gu *et al.*[7] modeled a free-floating space manipulator system as an extended system that was composed of a pseudo-arm representing the base motion resulting from six hypothetic passive joints and a real robot arm, and proposed an adaptive control scheme based on a normal form. Chen[8] studied the adaptive and robust composite control of the base's attitude of space manipulator with prismatic joint and its arms. Later, Chen[9] studied the adaptive control of the base's attitude and its arm's joints of dual-arm space manipulator. Guo[10] demonstrated that the dynamic equations of a dual-arm space manipulator could be linearly dependent on a group of composite inertial parameters, proposed a

* Corresponding author. E-mail: cool09@163.com

https://doi.org/10.1017/S0263574716000801 Published online by Cambridge University Press

robust control for such a system with uncertain inertial parameters. A robust controller, which could compensate external disturbances, was introduced by Chen.[11]

All of the above mentioned modeling and control methods for space manipulators assumed that arms mounted on their spacecraft are rigid. In practice light space manipulators need to be built, this can save launch cost and extend the orbit life. So, structural flexibility in the arms is a well-known problem, and various control strategies have been proposed.[12–23]

Joint elasticity is another confusion of large space manipulators.[24] Joint elasticity is more challenging than link flexibility in some cases.[25] There are considerable joint elasticity in space manipulators with planetary gear trains,[26] whereas these elastic behaviors are more serious in light manipulators with harmonic drives.[27] Due to high torque capability, reliable repeatability, wide working temperature range, low weight and compactness, harmonic drive mechanisms are becoming increasingly popular for space manipulators. Neglecting joint elasticity in control system design can lead to instability.[28] A passivity based control methodology for flexible joint manipulators to a simplified space shuttle RMS was proposed.[29] Hu *et al.*[30] studied a system consisting of several flexible joint space manipulator with closed kinematic chain constraints, and proposed a coordinated controller; this controller consisted of a position and internal force slow sub-controller and a joint elastic force fast sub-controller. An extended Kalman filter strategy to estimate state variables from noisy measurements in flexible joint space manipulators was presented by Ulrich *et al.*[31] Zhang *et al.* [32] proposed a method of adaptive fuzzy compensation and backstepping control for the precision trajectory tracking of flexible-joint space manipulator. The dynamic model of a space manipulator with flexible joints and friction was established, and an anti-windup nonlinear PD control was designed to avoid the torque saturation of the joints.[33] Xie *et al.*[34] proposed a singular perturbation fuzzy variable structure sliding mode controller to track inertial trajectory and suppress the elastic vibration of free-floating space manipulator system with flexible joints. Chen *et al.*[35] studied the dynamic modeling and singular perturbation neural network control of free-floating space robot with normal flexible joints and introduced a joint compensator to accommodate the equivalent joint flexibility of the joints. An adaptive trajectory control of space manipulators, which exhibited elastic vibrations in their joints and were subject to parametric uncertainties and modeling errors, was addressed.[36] Zou *et al.*[37] studied parameter identification and controller design for flexible joint of Chinese space manipulator and experiments were carried out to demonstrate it.

In all of the above control algorithms, space attitude angular velocities and joint velocities are available. Sometimes it may be impossible to measure these velocities directly, or it may be undesirable to do this.[38] For example, there might be noise in the signals measured by tachometers. Also, costs are increased owing to using more sensors. Yu and Chen[38] proposed a composite observer-based singular perturbation adaptive controller for a free-floating space manipulator with flexible joints and unknown physical parameters. In actual space manipulator, there often are external disturbance. In this paper, the external disturbance was taken into account, and the corresponding observer-based controller was studied.

In a free-floating space manipulator system, the spacecraft's position and attitude are not actively controlled during arm activity, this can conserve attitude control fuel, but the spacecraft will move freely in response to the dynamical disturbances caused by the arms' motions. However, the motion of free-floating spacecraft will disturb communication devices and solar panels mounted on it. Since communication devices and solar panels are more sensitive to the change of spacecraft's attitude than to that of spacecraft's position, it is important to study space manipulator with attitude controlled spacecraft (that is a free-flying space manipulator).[39,40] This paper deals with the problem of controlling a free-flying flexible-joint space manipulator with unknown payload parameters and bounded disturbances, which requires only angular displacement measurements. First, the dynamic equations of a free-flying space manipulator with two flexible revolute joints were derived by the momentum conservation law and the Lagrange equations. Second, a flexibility compensator was introduced to make the equivalent joint stiffness large enough, which made traditional singular perturbation approach applicable. Then, by singular perturbation theory, the system was disassembled into two subsystems, a slow subsystem and a flexible-joint fast subsystem. An observer-based composite robust controller was proposed; this controller consisted of a slow sub-controller and a fast sub-controller. To the slow subsystem, a sliding observer-based robust control algorithm was proposed. By optimal linear quadratic regulator method, the fast sub-controller was designed with the estimated velocity by linear observer. This fast sub-controller could stabilize the fast subsystem

https://doi.org/10.1017/S0263574716000801 Published online by Cambridge University Press

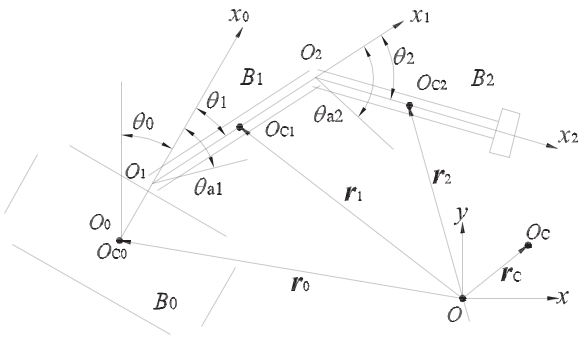


Fig. 1. A planar free-flying flexible-joint space manipulator.

around the equilibrium trajectory set up by the slow subsystem under the effect of the slow control. Finally, the numerical simulations were carried out, which showed that elastic joint vibrations had been stabilized effectively and good tracking performances had been achieved.

2. Dynamic Model of a Free-Flying Flexible-Joint Space Manipulator

The orbit manipulator system is modeled by a multi-body approach. The structure of the manipulator system is shown in Fig. 1. In this system, there are a rigid body satellite B_0, two rigid links B_1, B_2 (B_2 involves the payload) and two flexible joints. The links were connected in serial and are actuated by individual actuators. O_{Ci} is the mass center of B_i (i =0,1,2). O_0 coincides with O_{C0}. O_i (i =1,2) is the rotational center of the revolute joint between link B_{i-1} and link B_i. x_i (i = 1,2) is the symmetrical axis of link B_i. Other symbols are defined as follows:

(O–xy): Inertial coordinate frame of the system;
(O_i–$x_i\,y_i$): Local coordinate frame of B_i (i =0,1,2);
$\boldsymbol{e}_i$: Unit vector along the x_i axis;
l_0: Distance from point O to O_1;
d_i: Distance from point O_{Ci} to O_i(i =1,2);
l_i: Length of B_i (i =1,2) along the x_i axis;
m_i: Mass of B_i (i =0,1,2);
I_i: Inertial moment of B_i with respect to its mass center O_{Ci} (i =0,1,2);
I_{ai}: Inertial moment of the ith actuator;
O_C: Mass center of the entire system;
$\boldsymbol{r}_i$: Position vector of the mass center O_{Ci} of B_i (i =0,1,2) in (O–xy) frame;
$\boldsymbol{r}_C$: Position vector of the mass center O_C of the entire system in (O–xy) frame;
θ_0: Attitude angle of the base, which is the angle between the y axis and the x_0 axis;
θ_i: The ith link angular displacement (i =1,2), i.e., the angle between the x_{i-1} axis and the x_i axis;
θ_{ai}: The ith actuator angular displacement (i =1,2);
θ_{0d}: Desired attitude angle of the base;
θ_{id}: The desired ith link angular displacement (i =1,2);
θ_{aid}: The desired ith actuator angular displacement (i =1,2);
k_i: The ith joint stiffness (i =1,2);
N_i: Combined parameter of the system inertial parameters (i =0,1,2);
$\boldsymbol{q}_a$: The angular displacements vector of the actuator shaft angles ($\boldsymbol{q}_a = [\,\theta_{a1}\ \ \theta_{a2}\,]^{\mathrm{T}}$);
$\boldsymbol{q}_l$: The link angular displacements vector ($\boldsymbol{q}_l = [\ \theta_1\ \ \theta_2\,]^{\mathrm{T}}$);
$\boldsymbol{p}_0$: The initial momentum of the system;
T: The total kinetic energy of the system;
T_0: The base's kinetic energy;
T_i: The ith link's kinetic energy (i =1,2);
T_{ai}: The ith actuator's rotation kinetic energy (i =1,2);
V: The system's potential energy;
L: The system's Lagrangian;

https://doi.org/10.1017/S0263574716000801 Published online by Cambridge University Press

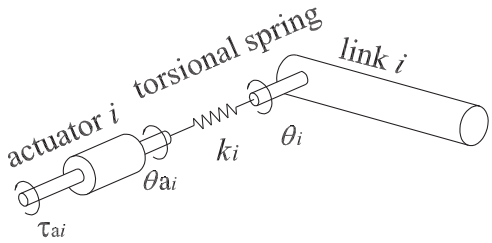


Fig. 2. Simple model of a flexible joint.

$\boldsymbol{q}_{bl}$: The angular displacements vector of the base and links ($\boldsymbol{q}_{bl} = [\,\theta_0\ \theta_1\ \theta_2\,]^{\mathrm{T}}$);
τ_0: The attitude control torque of the base;
τ_{ai} : The joint torque delivered by actuator i(i =1,2);
$\boldsymbol{\tau}_a$: The joint torque vector delivered by actuators $\boldsymbol{\tau}_a = [\,\boldsymbol{\tau}_{a1}\ \ \boldsymbol{\tau}_{a2}\,]^{\mathrm{T}}$;
$\boldsymbol{K}_{fj}$: The joint stiffness matrix $\boldsymbol{K}_{fj} = \mathrm{diag}[k_1\ k_2]$;
$\boldsymbol{\tau}_d$: Any additional disturbances and unmodeled dynamics;
$\|\boldsymbol{B}\|$: The induced norm of matrix $\boldsymbol{B}$ ($\|\boldsymbol{B}\| = \sqrt{\lambda_{\max}\{\boldsymbol{B}^{\mathrm{T}}\boldsymbol{B}\}}$);
$\lambda_{\max}()$: The maximum eigenvalue of ();
B_{min}: The minimum eigenvalue of positive definite matrix $\boldsymbol{B}(\boldsymbol{v})$(for all $\boldsymbol{v}$);
B_{max}: The maximum eigenvalue of positive definite matrix $\boldsymbol{B}(\boldsymbol{v})$(for all $\boldsymbol{v}$);
$\|\boldsymbol{B}\|_F$: Frobenius norm of matrix $\boldsymbol{B}$;
$\dot{(\,)}$: The first time derivative of ();
$\ddot{(\,)}$: The second time derivative of ();
$\hat{(\,)}$: The estimate of ();
$\bar{(\,)}$:The corresponding variable of () in the slow subsystem.

The ith flexible joint is shown schematically in Fig. 2. Each joint was dynamically simplified as a linear torsion spring; this spring is a connector between the actuator rotor and the link.

Since this paper is focused on the course of the system's pursuing the target, in this course external torques and forces were not applied to the system, equilibrium of forces and momentum conservation strictly hold.

The multi-body system is considered two-dimensional, so each joint's motion was restricted to rotate in one degree of freedom.

Referring to ref. [41], the damping was ignored and the stiffness of each joint was assumed to be constant.

Thus, position vectors $\boldsymbol{r}_i$ (i =1,2) are

$$\boldsymbol{r}_1 = \boldsymbol{r}_0 + l_0\boldsymbol{e}_0 + d_1\boldsymbol{e}_1 \tag{1}$$

$$\boldsymbol{r}_2 = \boldsymbol{r}_0 + l_0\boldsymbol{e}_0 + l_1\boldsymbol{e}_1 + d_2\boldsymbol{e}_2 \tag{2}$$

where

$$\begin{aligned}
\boldsymbol{e}_0 &= [\sin(\theta_0)\ \cos(\theta_0)]^{\mathrm{T}},\\
\boldsymbol{e}_1 &= [\sin(\theta_0+\theta_1)\ \cos(\theta_0+\theta_1)]^{\mathrm{T}},\\
\boldsymbol{e}_2 &= [\sin(\theta_0+\theta_1+\theta_2)\ \cos(\theta_0+\theta_1+\theta_2)]^{\mathrm{T}}.
\end{aligned}$$

Differentiating Eqs. (1) and (2) with respect to time t, velocity vectors $\dot{\boldsymbol{r}}_i (i = 1, 2)$ are

$$\dot{\boldsymbol{r}}_1 = \dot{\boldsymbol{r}}_0 + l_0\dot{\boldsymbol{e}}_0 + d_1\dot{\boldsymbol{e}}_1 \tag{3}$$

$$\dot{\boldsymbol{r}}_2 = \dot{\boldsymbol{r}}_0 + l_0\dot{\boldsymbol{e}}_0 + l_1\dot{\boldsymbol{e}}_1 + d_2\dot{\boldsymbol{e}}_2 \tag{4}$$

where

$$\begin{aligned}
\dot{\boldsymbol{e}}_0 &= \dot{\theta}_0[\cos(\theta_0)\ -\sin(\theta_0)]^{\mathrm{T}},\\
\dot{\boldsymbol{e}}_1 &= \left(\dot{\theta}_0+\dot{\theta}_1\right)[\cos(\theta_0+\theta_1)\ -\sin(\theta_0+\theta_1)]^{\mathrm{T}},\\
\dot{\boldsymbol{e}}_2 &= \left(\dot{\theta}_0+\dot{\theta}_1+\dot{\theta}_2\right)[\cos(\theta_0+\theta_1+\theta_2)\ -\sin(\theta_0+\theta_1+\theta_2)]^{\mathrm{T}}.
\end{aligned}$$

https://doi.org/10.1017/S0263574716000801 Published online by Cambridge University Press

Then, position vector $\boldsymbol{r}_C$ of the system's mass center O_C is

$$\boldsymbol{r}_C = \frac{\sum_{i=0}^{2} m_i \boldsymbol{r}_i}{M} \tag{5}$$

where

$$M = m_0 + m_1 + m_2.$$

Utilize Eqs. (1), (2) and (5), then $\boldsymbol{r}_i$ (i =0,1,2) are expressed as

$$\boldsymbol{r}_0 = \boldsymbol{r}_C + N_0\boldsymbol{e}_0 + N_1\boldsymbol{e}_1 + N_2\boldsymbol{e}_2 \tag{6}$$

$$\boldsymbol{r}_1 = \boldsymbol{r}_C + (N_0 + l_0)\,\boldsymbol{e}_0 + (N_1 + d_1)\,\boldsymbol{e}_1 + N_2\boldsymbol{e}_2 \tag{7}$$

$$\boldsymbol{r}_2 = \boldsymbol{r}_C + (N_0 + l_0)\,\boldsymbol{e}_0 + (N_1 + l_1)\,\boldsymbol{e}_1 + (N_2 + d_2)\,\boldsymbol{e}_2 \tag{8}$$

where $N_0 = -\frac{(m_1+m_2)}{M} l_0$, $N_1 = -\frac{(m_1 d_1 + m_2 l_1)}{M}$, $N_2 = -\frac{m_2 d_2}{M}$.

Neglecting the microgravity, the system's momentum is conserved during the operation. Then, Eq. (9) is obtained:

$$\sum_{i=0}^{2} m_i \dot{\boldsymbol{r}}_i = M\dot{\boldsymbol{r}}_C = \boldsymbol{p}_0. \tag{9}$$

Substitute Eqs. (3) and (4) into Eq. (9), then $\dot{\boldsymbol{r}}_0$ is

$$\dot{\boldsymbol{r}}_0 = \dot{\boldsymbol{r}}_C + N_0\dot{\boldsymbol{e}}_0 + N_1\dot{\boldsymbol{e}}_1 + N_2\dot{\boldsymbol{e}}_2. \tag{10}$$

Substitute Eq. (10) into Eqs. (3) and (4), then Eqs. (11) and (12) are obtained:

$$\dot{\boldsymbol{r}}_1 = \dot{\boldsymbol{r}}_C + (N_0 + l_0)\,\dot{\boldsymbol{e}}_0 + (N_1 + d_1)\,\dot{\boldsymbol{e}}_1 + N_2\dot{\boldsymbol{e}}_2 \tag{11}$$

$$\dot{\boldsymbol{r}}_2 = \dot{\boldsymbol{r}}_C + (N_0 + l_0)\,\dot{\boldsymbol{e}}_0 + (N_1 + l_1)\,\dot{\boldsymbol{e}}_1 + (N_2 + d_2)\,\dot{\boldsymbol{e}}_2. \tag{12}$$

Since the system initial momentum is $\boldsymbol{p}_0$, velocity vectors $\dot{\boldsymbol{r}}_i (i = 0, 1, 2)$ are

$$\dot{\boldsymbol{r}}_0 = \frac{\boldsymbol{p}_0}{M} + N_0\dot{\boldsymbol{e}}_0 + N_1\dot{\boldsymbol{e}}_1 + N_2\dot{\boldsymbol{e}}_2 \tag{13}$$

$$\dot{\boldsymbol{r}}_1 = \frac{\boldsymbol{p}_0}{M} + (N_0 + l_0)\,\dot{\boldsymbol{e}}_0 + (N_1 + d_1)\,\dot{\boldsymbol{e}}_1 + N_2\dot{\boldsymbol{e}}_2 \tag{14}$$

$$\dot{\boldsymbol{r}}_2 = \frac{\boldsymbol{p}_0}{M} + (N_0 + l_0)\,\dot{\boldsymbol{e}}_0 + (N_1 + l_1)\,\dot{\boldsymbol{e}}_1 + (N_2 + d_2)\,\dot{\boldsymbol{e}}_2. \tag{15}$$

By the quality concentrated method,[41] the translation kinetic energy of the actuator can be transferred to the link connected with it. Therefore, the total kinetic energy of the free-flying flexible-joint space manipulator T is

$$T = T_0 + \sum_{i=1}^{2} (T_i + T_{ai}) \tag{16}$$

where $T_0 = \frac{1}{2}(m_0\dot{\boldsymbol{r}}_0^2 + I_0\dot{\theta}_0^2)$, $T_1 = \frac{1}{2}(m_1\dot{\boldsymbol{r}}_1^2 + I_1(\dot{\theta}_0 + \dot{\theta}_1)^2)$, $T_2 = \frac{1}{2}(m_2\dot{\boldsymbol{r}}_2^2 + I_2(\dot{\theta}_0 + \dot{\theta}_1 + \dot{\theta}_2)^2)$, and $T_{ai} = \frac{1}{2} I_{ai}\dot{\theta}_{ai}^2 (i = 1, 2)$.

https://doi.org/10.1017/S0263574716000801 Published online by Cambridge University Press

Neglect the microgravity, the system's potential energy is

$$V = \frac{1}{2}\sum_{i=1}^{2} k_i(\theta_i - \theta_{ai})^2 \tag{17}$$

where k_i is the ith flexible-joint's stiffness. Therefore, the system's Lagrangian $L = T - V$ is obtained from Eqs. (16) and (17). Then, by the Lagrange equations, the dynamic equations of the free-flying flexible-joint space manipulator are as follows:

$$\boldsymbol{D}\left(\boldsymbol{q}_{bl}\right)\ddot{\boldsymbol{q}}_{bl} + \boldsymbol{h}\left(\boldsymbol{q}_{bl}, \dot{\boldsymbol{q}}_{bl}\right)\dot{\boldsymbol{q}}_{bl} + \boldsymbol{\tau}_d\left(\boldsymbol{q}_{bl}, \dot{\boldsymbol{q}}_{bl}, t\right) = \begin{bmatrix}\tau_0 \\ -\boldsymbol{K}_{fj}\left(\boldsymbol{q}_l - \boldsymbol{q}_a\right)\end{bmatrix} \tag{18a}$$

$$\boldsymbol{J}_a\ddot{\boldsymbol{q}}_a = \boldsymbol{K}_{fj}\left(\boldsymbol{q}_l - \boldsymbol{q}_a\right) + \boldsymbol{\tau}_a \tag{18b}$$

where positive-definite matrices $\boldsymbol{D}(\boldsymbol{q}_{bl}) \in \mathbf{R}^{3\times3}$ and $\boldsymbol{J}_a \in \mathbf{R}^{2\times2}$ are the links and actuators inertia matrices, respectively; $\boldsymbol{h}(\boldsymbol{q}_{bl}, \dot{\boldsymbol{q}}_{bl}) \in \mathbf{R}^{3\times3}$ is the Coriolis/centrifugal matrix;$\tau_0$is the attitude control torque of the base; $\boldsymbol{\tau}_a \in \mathbf{R}^2$ is the joint torque/force delivered by actuators; and $\boldsymbol{K}_{fj}(\boldsymbol{q}_l - \boldsymbol{q}_a) \in \mathbf{R}^2$ is the elastic forces vectors at joints. See Appendix A for details of $\boldsymbol{D}(\boldsymbol{q}_{bl})$, $\boldsymbol{J}_a$ and $\boldsymbol{h}(\boldsymbol{q}_{bl}, \dot{\boldsymbol{q}}_{bl})$.

3. Two-Time Scale Control

An alternative nonlinear approach to trajectory tracking of a free-flying flexible-joint space manipulator can be designed by the different time scales between the rigid dynamics and the flexible-joint system dynamics. This can be made by singular perturbation approach.[42]

Let $\boldsymbol{\tau}_l = -\boldsymbol{K}_{fj}(\boldsymbol{q}_l - \boldsymbol{q}_a)$, so $\ddot{\boldsymbol{q}}_a = \boldsymbol{K}_{fj}{}^{-1}\ddot{\boldsymbol{\tau}}_l + \ddot{\boldsymbol{q}}_l$, then the dynamic equations of the system are

$$\boldsymbol{D}\left(\boldsymbol{q}_{bl}\right)\ddot{\boldsymbol{q}}_{bl} + \boldsymbol{h}\left(\boldsymbol{q}_{bl}, \dot{\boldsymbol{q}}_{bl}\right)\dot{\boldsymbol{q}}_{bl} + \boldsymbol{\tau}_d\left(\boldsymbol{q}_{bl}, \dot{\boldsymbol{q}}_{bl}, t\right) = \begin{bmatrix}\tau_0 \\ \boldsymbol{\tau}_l\end{bmatrix} \tag{19a}$$

$$\boldsymbol{J}_a\boldsymbol{K}_{fj}{}^{-1}\ddot{\boldsymbol{\tau}}_l + \boldsymbol{\tau}_l = \boldsymbol{\tau}_a - \boldsymbol{J}_a\ddot{\boldsymbol{q}}_l. \tag{19b}$$

The traditional singular perturbation approach is applicable to manipulators whose joint stiffness is large enough.[43] However, the joint stiffness of the actual space manipulator is always not large enough, a flexibility compensator is introduced here. This compensator is proposed by Liu *et al.*[44]

Define $\boldsymbol{\tau}_a$ as

$$\boldsymbol{\tau}_a = \boldsymbol{K}_n\boldsymbol{\tau}_n + \boldsymbol{\tau}_c \tag{20}$$

where $\boldsymbol{K}_n \in R^{2\times2}$ is determined later, $\boldsymbol{\tau}_n$ is a new controller and $\boldsymbol{\tau}_c$ is a flexibility compensator.

Then, Eq. (21) is obtained from Eq. (19b):

$$\boldsymbol{J}_a\boldsymbol{K}_{fj}{}^{-1}\ddot{\boldsymbol{\tau}}_l + \boldsymbol{\tau}_l = \boldsymbol{K}_n\left(\boldsymbol{\tau}_n - \boldsymbol{K}_n^{-1}\boldsymbol{J}_a\ddot{\boldsymbol{q}}_l\right) + \boldsymbol{\tau}_c. \tag{21}$$

Let

$$\boldsymbol{\tau}_c = -\boldsymbol{K}_c\boldsymbol{\tau}_l \tag{22}$$

where $\boldsymbol{K}_c \in R^{2\times2}$ is a positive-definite diagonal flexibility compensation matrix. Then, Eq. (23) is derived from Eq. (21):

$$\boldsymbol{J}_a\boldsymbol{K}_{fj}{}^{-1}\ddot{\boldsymbol{\tau}}_l + \left(\boldsymbol{E}_1 + \boldsymbol{K}_c\right)\boldsymbol{\tau}_l = \boldsymbol{K}_n\left(\boldsymbol{\tau}_n - \boldsymbol{K}_n^{-1}\boldsymbol{J}_a\ddot{\boldsymbol{q}}_l\right) \tag{23}$$

where$\boldsymbol{E}_1$is a second-order identity matrix.

Let $\boldsymbol{K}_n = \boldsymbol{E}_1 + \boldsymbol{K}_c$, Eq. (23) is rewritten as

$$\boldsymbol{J}_a\boldsymbol{K}_{fjc}{}^{-1}\ddot{\boldsymbol{\tau}}_l + \boldsymbol{\tau}_l = \boldsymbol{\tau}_n - \boldsymbol{K}_n^{-1}\boldsymbol{J}_a\ddot{\boldsymbol{q}}_l \tag{24}$$

https://doi.org/10.1017/S0263574716000801 Published online by Cambridge University Press

where $\boldsymbol{K}_{fjc} = \boldsymbol{K}_{fj}\boldsymbol{K}_n$ is the equivalent joint stiffness. Obviously, $\boldsymbol{K}_{fjc}$ can be adjusted to any expected value as long as $\boldsymbol{K}_n$ is reasonably taken.

Let $\boldsymbol{K}_\mu = \mu^2\boldsymbol{K}_{fjc}$, where the small constant μ is the singular perturbation parameter. The flexible-joint subsystem (24) becomes

$$\mu^2\boldsymbol{J}_a\ddot{\boldsymbol{\tau}}_l + \boldsymbol{K}_\mu\boldsymbol{\tau}_l = \boldsymbol{K}_\mu\left(\boldsymbol{\tau}_n - \boldsymbol{K}_n^{-1}\boldsymbol{J}_a\ddot{\boldsymbol{q}}_l\right). \tag{25}$$

When $\mu \to 0$, Eq. (25) becomes

$$\bar{\boldsymbol{\tau}}_l = \bar{\boldsymbol{\tau}}_n - \boldsymbol{K}_n^{-1}\boldsymbol{J}_a\ddot{\bar{\boldsymbol{q}}}_l \tag{26}$$

and at the same time Eq. (19a) becomes

$$\boldsymbol{D}\left(\bar{\boldsymbol{q}}_{bl}\right)\ddot{\bar{\boldsymbol{q}}}_{bl} + \boldsymbol{h}\left(\bar{\boldsymbol{q}}_{bl}, \dot{\bar{\boldsymbol{q}}}_{bl}\right)\dot{\bar{\boldsymbol{q}}}_{bl} + \boldsymbol{\tau}_d\left(\bar{\boldsymbol{q}}_{bl}, \dot{\bar{\boldsymbol{q}}}_{bl}, t\right) = \begin{bmatrix}\bar{\tau}_0 \\ \bar{\boldsymbol{\tau}}_l\end{bmatrix}. \tag{27}$$

Substitute Eq. (26) into Eq. (27), then the dynamic equation of the slow subsystem is obtained as

$$\left(\boldsymbol{D}\left(\bar{\boldsymbol{q}}_{bl}\right) + \begin{bmatrix}\boldsymbol{0} & \boldsymbol{0} \\ \boldsymbol{0} & \boldsymbol{K}_n^{-1}\boldsymbol{J}_a\end{bmatrix}\right)\ddot{\bar{\boldsymbol{q}}}_{bl} + \boldsymbol{h}\left(\bar{\boldsymbol{q}}_{bl}, \dot{\bar{\boldsymbol{q}}}_{bl}\right)\dot{\bar{\boldsymbol{q}}}_{bl} + \boldsymbol{\tau}_d\left(\bar{\boldsymbol{q}}_{bl}, \dot{\bar{\boldsymbol{q}}}_{bl}, t\right) = \begin{bmatrix}\bar{\tau}_0 \\ \bar{\boldsymbol{\tau}}_n\end{bmatrix}. \tag{28}$$

The slow subsystem represents the rigid part of the system. If the joint stiffness is large enough, then $\boldsymbol{K}_n = \boldsymbol{E}_1$, and $\boldsymbol{K}_c$ is second-order zero matrix.

Then, let $\boldsymbol{\zeta}_1 = \boldsymbol{\tau}_l - \bar{\boldsymbol{\tau}}_l$ and $\zeta_2 = \mu\dot{\boldsymbol{\tau}}_l$, a fast-time scale $t_f = \frac{t-t_0}{\mu}$ is introduced. Therefore, the flexible-joint fast subsystem (25) is transformed into

$$\frac{\mathrm{d}\zeta_1}{\mathrm{d}t_f} = \zeta_2 - \mu\dot{\bar{\boldsymbol{\tau}}}_l \tag{29}$$

$$\frac{\mathrm{d}\zeta_2}{\mathrm{d}t_f} = \boldsymbol{J}_a^{-1}\boldsymbol{K}_\mu\left(\boldsymbol{\tau}_n - \boldsymbol{K}_n^{-1}\boldsymbol{J}_a\ddot{\boldsymbol{q}}_l - \zeta_1 - \bar{\boldsymbol{\tau}}_l\right). \tag{30}$$

Define $\boldsymbol{\tau}_n = \bar{\boldsymbol{\tau}}_n + \boldsymbol{\tau}_{nf}$, where $\bar{\boldsymbol{\tau}}_n$ is the slow link control component and $\boldsymbol{\tau}_{nf}$ is a flexible-joint fast control component. when $\mu \to 0$, and using Eq. (26), the flexible-joint fast subsystem dynamic equations (29) and (30) become

$$\frac{\mathrm{d}\boldsymbol{\zeta}}{\mathrm{d}t_f} = \boldsymbol{A}\boldsymbol{\zeta} + \boldsymbol{B}\boldsymbol{\tau}_{nf} \tag{31}$$

where $\boldsymbol{\zeta} = [\,\boldsymbol{\zeta}_1^{\mathrm{T}}\ \boldsymbol{\zeta}_2^{\mathrm{T}}\,]^{\mathrm{T}}$, $\boldsymbol{A} = \begin{bmatrix}\boldsymbol{0} \in \mathbf{R}^{2\times2} & \boldsymbol{E}_1 \in \mathbf{R}^{2\times2} \\ -\boldsymbol{J}_a^{-1}\boldsymbol{K}_\mu \in \mathbf{R}^{2\times2} & \boldsymbol{0} \in \mathbf{R}^{2\times2}\end{bmatrix}$ and $\boldsymbol{B} = \begin{bmatrix}\boldsymbol{0} \in \mathbf{R}^{2\times2} \\ \boldsymbol{J}_a^{-1}\boldsymbol{K}_\mu\end{bmatrix}$.

3.1. Robust control design for the slow subsystem

The dynamic equation of the slow subsystem (28) is written as

$$\bar{\boldsymbol{D}}\left(\bar{\boldsymbol{q}}_{bl}\right)\ddot{\bar{\boldsymbol{q}}}_{bl} + \bar{\boldsymbol{h}}\left(\bar{\boldsymbol{q}}_{bl}, \dot{\bar{\boldsymbol{q}}}_{bl}\right)\dot{\bar{\boldsymbol{q}}}_{bl} + \boldsymbol{\tau}_d\left(\bar{\boldsymbol{q}}_{bl}, \dot{\bar{\boldsymbol{q}}}_{bl}, t\right) = \bar{\boldsymbol{\tau}} \tag{32}$$

where $\bar{\boldsymbol{D}}(\bar{\boldsymbol{q}}_{bl}) = \boldsymbol{D}(\bar{\boldsymbol{q}}_{bl}) + \begin{bmatrix}\boldsymbol{0} & \boldsymbol{0} \\ \boldsymbol{0} & \boldsymbol{K}_n^{-1}\boldsymbol{J}_a\end{bmatrix}$, $\bar{\boldsymbol{h}}(\bar{\boldsymbol{q}}_{bl}, \dot{\bar{\boldsymbol{q}}}_{bl}) = \boldsymbol{h}(\bar{\boldsymbol{q}}_{bl}, \dot{\bar{\boldsymbol{q}}}_{bl})$, $\bar{\boldsymbol{\tau}} = \begin{bmatrix}\bar{\tau}_0 \\ \bar{\boldsymbol{\tau}}_n\end{bmatrix}$, $\bar{\boldsymbol{\tau}}_n = \begin{bmatrix}\bar{\tau}_1 \\ \bar{\tau}_2\end{bmatrix}$, τ_0 is the attitude control torque of the base for the slow subsystem and $\bar{\tau}_i (i = 1, 2)$ is the ith joint control torque for the slow subsystem.

When $\bar{\boldsymbol{h}}(\bar{\boldsymbol{q}}_{bl}, \dot{\bar{\boldsymbol{q}}}_{bl})$ is suitably defined, matrix $\dot{\bar{\boldsymbol{D}}} - 2\bar{\boldsymbol{h}}$ is skew symmetric:[45,46]

$$\bar{h}_{ij} = \sum_{k=1}^{3}\frac{1}{2}\left(\frac{\partial\bar{D}_{ij}}{\partial\bar{q}_{blk}} + \frac{\partial\bar{D}_{ik}}{\partial\bar{q}_{blj}} - \frac{\partial\bar{D}_{jk}}{\partial\bar{q}_{bli}}\right)\dot{\bar{q}}_{blk}.$$

https://doi.org/10.1017/S0263574716000801 Published online by Cambridge University Press

Introduce the state vector $\boldsymbol{x}_1 = \bar{\boldsymbol{q}}_{bl}, \boldsymbol{x}_2 = \dot{\bar{\boldsymbol{q}}}_{bl}$, the state-space representation of the slow subsystem dynamic equation (32) is

$$\begin{cases} \dot{\boldsymbol{x}}_1 = \boldsymbol{x}_2 \\ \dot{\boldsymbol{x}}_2 = \bar{\boldsymbol{D}}^{-1}(\boldsymbol{x}_1)\left(\bar{\boldsymbol{\tau}} - \bar{\boldsymbol{h}}(\boldsymbol{x}_1, \boldsymbol{x}_2)\boldsymbol{x}_2 - \boldsymbol{\tau}_d\right) \end{cases}. \tag{33}$$

Define the model error

$$\begin{cases} \tilde{\bar{\boldsymbol{D}}} = \bar{\boldsymbol{D}} - \hat{\bar{\boldsymbol{D}}} \\ \tilde{\bar{\boldsymbol{h}}} = \bar{\boldsymbol{h}} - \hat{\bar{\boldsymbol{h}}} \end{cases} \tag{34}$$

where $\hat{\bar{\boldsymbol{D}}}, \hat{\bar{\boldsymbol{h}}}$ are the estimates of $\bar{\boldsymbol{D}}, \bar{\boldsymbol{h}}$.

The manipulator model (32) has the following properties.[47–49]

Property 1. $\bar{\boldsymbol{D}}(\bar{\boldsymbol{q}}_{bl})$ is a positive definite symmetric matrix, and both $\bar{\boldsymbol{D}}(\bar{\boldsymbol{q}}_{bl})$ and $\bar{\boldsymbol{D}}^{-1}(\bar{\boldsymbol{q}}_{bl})$ are uniformly bounded as function of $\bar{\boldsymbol{q}}_{bl}$.

Property 2. For an arbitrary vector $\mathbf{z} \in R^3$, the following equation is satisfied:

$$z^{\mathrm{T}}\bar{\boldsymbol{h}}z = \frac{1}{2}\mathbf{z}^{\mathrm{T}}\dot{\bar{\boldsymbol{D}}}z.$$

Property 3. The vector $\bar{\boldsymbol{h}}(\bar{\boldsymbol{q}}_{bl}, \dot{\bar{\boldsymbol{q}}}_{bl})\dot{\bar{\boldsymbol{q}}}_{bl}$ satisfies

$$\bar{\boldsymbol{h}}(\bar{\boldsymbol{q}}_{bl}, v)z = \boldsymbol{h}(\bar{\boldsymbol{q}}_{bl}, z)v \ \forall \bar{\boldsymbol{q}}_{bl}, \boldsymbol{v}, z \in R^3.$$

Property 4. The matrix $\bar{\boldsymbol{h}}(\bar{\boldsymbol{q}}_{bl}, \dot{\bar{\boldsymbol{q}}}_{bl})$ satisfies

$$\begin{aligned} &\bar{\boldsymbol{h}}(\bar{\boldsymbol{q}}_{bl}, \boldsymbol{v}+z) = \bar{\boldsymbol{h}}(\bar{\boldsymbol{q}}_{bl}, \boldsymbol{v}) + \bar{\boldsymbol{h}}(\bar{\boldsymbol{q}}_{bl}, z) \quad \forall \bar{\boldsymbol{q}}_{bl}, \boldsymbol{v}, z \in R^3 \\ &\zeta_{\bar{h}min}\|\boldsymbol{v}\| \le \left\|\bar{\boldsymbol{h}}(\bar{\boldsymbol{q}}_{bl}, \boldsymbol{v})\right\| \le \zeta_{\bar{h}max}\|\boldsymbol{v}\| \end{aligned}$$

where $\zeta_{\bar{h}max}$ and $\zeta_{\bar{h}min}$ are positive constants.

The following assumptions were made for the slow subsystem.

Assumption 1. $\hat{\bar{\boldsymbol{D}}}(\bar{\boldsymbol{q}}_{bl})$ is a positive definite symmetric matrix, and both $\hat{\bar{\boldsymbol{D}}}(\bar{\boldsymbol{q}}_{bl})$ and $\hat{\bar{\boldsymbol{D}}}^{-1}(\bar{\boldsymbol{q}}_{bl})$ are uniformly bounded as function of $\bar{\boldsymbol{q}}_{bl}$.

$$\hat{\bar{D}}_{min} \le \left\|\hat{\bar{\boldsymbol{D}}}(\bar{\boldsymbol{q}}_{bl})\right\|_F \le \sqrt{3}\hat{\bar{D}}_{max}.$$

Assumption 2. The desired trajectory signals $\boldsymbol{q}_d(t)$, $\dot{\boldsymbol{q}}_d(t)$ and $\ddot{\boldsymbol{q}}_d(t)$ are upper bounded, and their upper bounds are known.

Assumption 3. The lower bound $\tilde{\bar{D}}_{min}$ and $\tilde{\bar{h}}_{min}$ of $\tilde{\bar{\boldsymbol{D}}}$ and $\tilde{\bar{\boldsymbol{h}}}$ are positive constants. $\|\boldsymbol{\tau}_d(\bar{\boldsymbol{q}}_{bl}, \dot{\bar{\boldsymbol{q}}}_{bl}, t)\| \le \zeta_d$, and ζ_d is a known positive constant.

Using Property 1 and Assumption 1, (35) is obtained as follows:

$$\left\|\bar{\boldsymbol{D}}^{-1}(\bar{\boldsymbol{q}}_{bl}) - \hat{\bar{\boldsymbol{D}}}^{-1}(\bar{\boldsymbol{q}}_{bl})\right\|_F \le \zeta_{\tilde{\bar{D}}^{-1}} \tag{35}$$

where $\zeta_{\tilde{\bar{D}}^{-1}} = \max\left(\left|\frac{1}{\tilde{\bar{D}}_{min}} - \frac{1}{\sqrt{3}\hat{\bar{D}}_{max} + \tilde{\bar{D}}_{max}}\right|, \left|\frac{1}{\sqrt{3}\hat{\bar{D}}_{max}} - \frac{1}{\tilde{\bar{D}}_{min} + \hat{\bar{D}}_{min}}\right|\right)$.

https://doi.org/10.1017/S0263574716000801 Published online by Cambridge University Press

3.1.1. Dynamic sliding observer for the slow subsystem.

The dynamic sliding observer (36) is proposed as follows:

$$\begin{cases} \dot{\hat{\boldsymbol{x}}}_1 = \hat{\boldsymbol{x}}_2 + \boldsymbol{\Lambda}_1 \mathrm{sgn}(\boldsymbol{x}_1 - \hat{\boldsymbol{x}}_1) \\ \dot{\hat{\boldsymbol{x}}}_2 = \hat{\bar{\boldsymbol{D}}}^{-1}(\boldsymbol{x}_1)\left(\bar{\boldsymbol{\tau}} - \hat{\bar{\boldsymbol{h}}}(\boldsymbol{x}_1, \hat{\boldsymbol{x}}_2)\hat{\boldsymbol{x}}_2\right) + \boldsymbol{\Lambda}_2 \,\mathrm{sgn}\,(\boldsymbol{x}_1 - \hat{\boldsymbol{x}}_1) + \boldsymbol{\eta}\,\mathrm{sgn}\,(\boldsymbol{x}_2 - \hat{\boldsymbol{x}}_2) \end{cases} \tag{36}$$

where $\hat{\boldsymbol{x}}_1$ and $\hat{\boldsymbol{x}}_2$ are estimates of $\boldsymbol{x}_1$ and $\boldsymbol{x}_2$, respectively, sgn(·)is the sign function, $\boldsymbol{\eta} = \mathrm{diag}(\eta^1, \eta^2, \eta^3)$ is given in the following, $\boldsymbol{\Lambda}_j = \mathrm{diag}(\gamma_j^1, \gamma_j^2, \gamma_j^3)$ $j = 1, 2$.

Then, the observation error dynamic of the slow subsystem is derived from Eqs. (33) and (36):

$$\begin{cases} \dot{\tilde{\boldsymbol{x}}}_1 = \tilde{\boldsymbol{x}}_2 - \boldsymbol{\Lambda}_1 \mathrm{sgn}(\boldsymbol{x}_1 - \hat{\boldsymbol{x}}_1) \\ \dot{\tilde{\boldsymbol{x}}}_2 = \bar{\boldsymbol{D}}^{-1}(\boldsymbol{x}_1)\left(\bar{\boldsymbol{\tau}} - \bar{\boldsymbol{h}}(\boldsymbol{x}_1, \boldsymbol{x}_2)\boldsymbol{x}_2 - \boldsymbol{\tau}_d\right) - \hat{\bar{\boldsymbol{D}}}^{-1}(\boldsymbol{x}_1)\left(\bar{\boldsymbol{\tau}} - \hat{\bar{\boldsymbol{h}}}(\boldsymbol{x}_1, \hat{\boldsymbol{x}}_2)\hat{\boldsymbol{x}}_2\right) \\ \qquad -\boldsymbol{\Lambda}_2 \mathrm{sgn}(\boldsymbol{x}_1 - \hat{\boldsymbol{x}}_1) - \boldsymbol{\eta}\mathrm{sgn}(\boldsymbol{x}_2 - \hat{\boldsymbol{x}}_2) \end{cases} \tag{37}$$

where $\tilde{\boldsymbol{x}}_i = \boldsymbol{x}_i - \hat{\boldsymbol{x}}_i$, $i = 1, 2$.

Define $\boldsymbol{s}_1 = \tilde{\boldsymbol{x}}_1$ and introduce the following Lyapunov function:

$$V_1 = \frac{1}{2}\tilde{\boldsymbol{x}}_1^{\mathrm{T}}\tilde{\boldsymbol{x}}_1. \tag{38}$$

And assure $\dot{V}_1 < 0$, the surface $\boldsymbol{s}_1 = 0$ is attractive within the set defined by the following inequalities $\forall i \in \{1, 2, 3\}$:

$$\begin{array}{l} \mathrm{if}\tilde{x}_1^i > 0 \text{ then } \tilde{x}_2^i - \gamma_1^i < 0 \\ \mathrm{if}\tilde{x}_1^i < 0 \text{ then } \tilde{x}_2^i + \gamma_1^i > 0. \end{array} \tag{39}$$

When $\tilde{\boldsymbol{x}}_1 = \boldsymbol{0}$, since $\dot{\tilde{\boldsymbol{x}}}_1 = \boldsymbol{0}$, the equivalent switching vector $\tilde{\boldsymbol{x}}_2$ is expressed from Eq. (37) as

$$\tilde{\boldsymbol{x}}_2 = \boldsymbol{x}_2 - \hat{\boldsymbol{x}}_2 = \boldsymbol{\Lambda}_1 \mathrm{sgn}(\boldsymbol{x}_1 - \hat{\boldsymbol{x}}_1). \tag{40}$$

Theorem 1. Provided that the initial estimates of system (33) satisfy $\hat{\boldsymbol{x}}_1(0) = \boldsymbol{x}_1(0)$, the dynamic sliding observer (36) could ensure the norm $\|\tilde{\boldsymbol{x}}_2\|$of the velocity estimate errors $\tilde{\boldsymbol{x}}_2$ converges exponentially to a bounded region with radius δ.

Proof.

Introduce the following Lyapunov function:

$$V_2 = \frac{1}{2}\tilde{\boldsymbol{x}}_2^{\mathrm{T}}\boldsymbol{D}\tilde{\boldsymbol{x}}_2. \tag{41}$$

According to Eq. (37) and Properties 2-4, the time derivative of (41) is

$$\begin{aligned} \dot{V}_2 &= \tilde{\boldsymbol{x}}_2^{\mathrm{T}}\bar{\boldsymbol{D}}\dot{\tilde{\boldsymbol{x}}}_2 + \tfrac{1}{2}\tilde{\boldsymbol{x}}_2^{\mathrm{T}}\dot{\bar{\boldsymbol{D}}}\tilde{\boldsymbol{x}}_2 \\ &= \tilde{\boldsymbol{x}}_2^{\mathrm{T}}\bar{\boldsymbol{D}}\left\{\begin{array}{l} \left(\bar{\boldsymbol{D}}^{-1} - \hat{\bar{\boldsymbol{D}}}^{-1}\right)\left(\bar{\boldsymbol{\tau}} - \hat{\bar{\boldsymbol{h}}}(\boldsymbol{x}_1, \hat{\boldsymbol{x}}_2)\hat{\boldsymbol{x}}_2\right) - \bar{\boldsymbol{D}}^{-1}\tilde{\bar{\boldsymbol{h}}}(\boldsymbol{x}_1, \hat{\boldsymbol{x}}_2)\hat{\boldsymbol{x}}_2 \\ -\bar{\boldsymbol{D}}^{-1}\left(\left(\hat{\bar{\boldsymbol{h}}}(\boldsymbol{x}_1, \hat{\boldsymbol{x}}_2)\tilde{\boldsymbol{x}}_2 + \tilde{\bar{\boldsymbol{h}}}(\boldsymbol{x}_1, \hat{\boldsymbol{x}}_2)\tilde{\boldsymbol{x}}_2\right) - \bar{\boldsymbol{D}}^{-1}\boldsymbol{\tau}_d - \boldsymbol{\Lambda}_2\,\mathrm{sgn}\,(\boldsymbol{x}_1 - \hat{\boldsymbol{x}}_1) - \boldsymbol{\eta}\mathrm{sgn}(\boldsymbol{x}_2 - \hat{\boldsymbol{x}}_2)\right) \end{array}\right\}. \end{aligned} \tag{42}$$

By Eq. (42), the dynamic compensating gain η^i(i=1,2,3) is given as follows:

$$\begin{aligned} \eta_i &= \zeta_{\tilde{\bar{D}}^{-1}} \cdot (|\bar{\tau}_i| + \left\|\hat{\bar{\boldsymbol{h}}}(\boldsymbol{x}_1, \hat{\boldsymbol{x}}_2)\right\|_F |\hat{x}_{2i}|) + \frac{\zeta_{\tilde{\bar{h}}max}\|\hat{\boldsymbol{x}}_2\|}{\left\|\hat{\bar{\boldsymbol{D}}}\right\|_F + \tilde{\bar{D}}_{min}}|\hat{x}_{2i}| \\ &\le \zeta_{\tilde{\bar{D}}^{-1}} \cdot (|\bar{\tau}_i| + \left\|\hat{\bar{\boldsymbol{h}}}(\boldsymbol{x}_1, \hat{\boldsymbol{x}}_2)\right\|_F |\hat{x}_{2i}|) + \frac{\zeta_{\tilde{\bar{h}}max}\|\hat{\boldsymbol{x}}_2\|}{\left(\hat{\bar{D}}_{max}\right)_{min} + \tilde{\bar{D}}_{min}}|\hat{x}_{2i}| \end{aligned} \tag{43}$$

https://doi.org/10.1017/S0263574716000801 Published online by Cambridge University Press

From Eqs. (40), (42) and (43), $\dot{V}_2$ satisfies

$$\dot{V}_2 \leq \tilde{\boldsymbol{x}}_2^{\mathrm{T}} \{-\boldsymbol{\tau}_d - \left(\hat{\bar{\boldsymbol{h}}}(\boldsymbol{x}_1, \hat{\boldsymbol{x}}_2) + \tilde{\bar{\boldsymbol{h}}}(\boldsymbol{x}_1, \hat{\boldsymbol{x}}_2) + \bar{\boldsymbol{D}} \boldsymbol{\Lambda}_2 \boldsymbol{\Lambda}_1^{-1}\right) \tilde{\boldsymbol{x}}_2\}. \tag{44}$$

Define$(\zeta_{\tilde{\bar{h}}min} \|\hat{\boldsymbol{x}}_2\| - \|\hat{\bar{\boldsymbol{h}}}(\boldsymbol{x}_1, \hat{\boldsymbol{x}}_2)\|_F) I + (\|\hat{\bar{D}}\|_F + \tilde{\bar{D}}_{min}) \boldsymbol{\Lambda}_2 \boldsymbol{\Lambda}_1^{-1} = \boldsymbol{P}$, where $\boldsymbol{P} = p\boldsymbol{E}$ and $p > 1/4$, then $\dot{V}_2$ satisfies

$$\dot{V}_2 \leq -\tilde{\boldsymbol{x}}_2^{\mathrm{T}} \boldsymbol{\tau}_d - \tilde{\boldsymbol{x}}_2^{\mathrm{T}} \boldsymbol{P} \tilde{\boldsymbol{x}}_2 = -\left[\tilde{\boldsymbol{x}}_2^{\mathrm{T}}, \boldsymbol{\tau}_d^{\mathrm{T}}\right] \begin{bmatrix} \boldsymbol{P} & \boldsymbol{E}/2 \\ \boldsymbol{E}/2 & \boldsymbol{E} \end{bmatrix} \begin{bmatrix} \tilde{\boldsymbol{x}}_2 \\ \boldsymbol{\tau}_d \end{bmatrix} + \boldsymbol{\tau}_d^{\mathrm{T}} \boldsymbol{\tau}_d \leq -Q_{\min} \|\tilde{\boldsymbol{x}}_2\|^2 + (1 - Q_{\min}) \zeta_d^2 \tag{45}$$

where $\boldsymbol{Q} = \left[\begin{smallmatrix} \boldsymbol{P} & \boldsymbol{E}/2 \\ \boldsymbol{E}/2 & \boldsymbol{E} \end{smallmatrix}\right]$, $Q_{\min} < 1$, $\boldsymbol{E}$is a third-order identity matrix.

If $\|\tilde{\boldsymbol{x}}_2\| \geq \delta = \sqrt{\frac{1-Q_{\min}}{Q_{\min}}} \zeta_d$, $\dot{V}_2 \leq 0$, then according to Wit De,[50] the norm $\|\tilde{\boldsymbol{x}}_2\|$ of the velocity estimate errors $\tilde{\boldsymbol{x}}_2$ converges exponentially to a bounded region with radius δ. $\delta < \|\boldsymbol{\Lambda}_1\|$ is assured by choosing appropriate $\boldsymbol{\Lambda}_2$.

3.1.2. Dynamic sliding observer based robust controller of the slow subsystem.

Introduce the following Lyapunov function:

$$V = V_2 + V_3 = \frac{1}{2} \tilde{\boldsymbol{x}}_2^{\mathrm{T}} \bar{\boldsymbol{D}} \tilde{\boldsymbol{x}}_2 + \frac{1}{2} \boldsymbol{s}_2^{\mathrm{T}} \bar{\boldsymbol{D}} \boldsymbol{s}_2 \tag{46}$$

where sliding surface $\boldsymbol{s}_2 = \boldsymbol{e}_2 + L\boldsymbol{e}_1$, $\boldsymbol{e}_2 = \dot{\boldsymbol{q}}_{bld} - \boldsymbol{x}_2$, $L > 0$, $\boldsymbol{e}_1 = \boldsymbol{q}_{bld} - \boldsymbol{x}_1$ $\boldsymbol{q}_{bld} = [\theta_{0d}\ \theta_{1d}\ \theta_{2d}]^{\mathrm{T}}$, $\dot{\boldsymbol{q}}_{bld} = [\dot{\theta}_{0d}\ \dot{\theta}_{1d}\ \dot{\theta}_{2d}]^{\mathrm{T}}$.

The time-derivative of Eq. (46) is

$$\begin{aligned} \dot{V} &= \dot{V}_2 + \dot{V}_3 = \dot{V}_2 + \boldsymbol{s}_2^{\mathrm{T}} \bar{\boldsymbol{D}} \dot{\boldsymbol{s}}_2 + \tfrac{1}{2} \boldsymbol{s}_2^{\mathrm{T}} \dot{\bar{\boldsymbol{D}}} \boldsymbol{s}_2 \\ &= \tilde{\boldsymbol{x}}_2^{\mathrm{T}} \bar{\boldsymbol{D}} \dot{\tilde{\boldsymbol{x}}}_2 + \tfrac{1}{2} \tilde{\boldsymbol{x}}_2^{\mathrm{T}} \dot{\bar{\boldsymbol{D}}} \tilde{\boldsymbol{x}}_2 + \boldsymbol{s}_2^{\mathrm{T}} \left(\bar{\boldsymbol{D}} \ddot{\boldsymbol{q}}_{bld} + \bar{\boldsymbol{h}}(\boldsymbol{x}_1, \boldsymbol{x}_2) \left(\dot{\boldsymbol{q}}_{bld} + L\boldsymbol{e}_1\right) + \boldsymbol{\tau}_d + \bar{\boldsymbol{D}} L \boldsymbol{e}_2 - \bar{\boldsymbol{\tau}}\right). \end{aligned} \tag{47}$$

According to Eq. (47), the robust controller (48) is proposed as follows:

$$\begin{cases} \bar{\boldsymbol{\tau}} = \bar{\boldsymbol{\tau}}_{\mathrm{eq}} + \bar{\boldsymbol{\tau}}_R \\ \bar{\boldsymbol{\tau}}_{\mathrm{eq}} = \hat{\bar{\boldsymbol{D}}} \ddot{\boldsymbol{q}}_{bld} + \hat{\bar{\boldsymbol{h}}}(\boldsymbol{x}_1, \hat{\boldsymbol{x}}_2) \left(\dot{\boldsymbol{q}}_{bld} + L\boldsymbol{e}_1\right) + \hat{\bar{\boldsymbol{D}}} L \hat{\boldsymbol{e}}_2 + \varepsilon \boldsymbol{s}_2 \\ \bar{\boldsymbol{\tau}}_R = \zeta_R \mathrm{sgn}(\boldsymbol{s}_2) \end{cases} \tag{48}$$

where $\hat{\boldsymbol{e}}_2 = \dot{\boldsymbol{q}}_{bld} - \hat{\boldsymbol{x}}_2$, ζ_R is given in the following, $\varepsilon \geq 0$.

Theorem 2. Properties 1-4 are satisfied in subsystem (33) with unknown payload parameters and bounded disturbances, and then the proposed robust observer-controller (36) and (48) could guarantee *locally uniform ultimate* boundedness for the tracking errors of the system.

Proof.

By Eq. (48), Eq. (47) becomes

$$\dot{V} = \tilde{\boldsymbol{x}}_2^{\mathrm{T}} \bar{\boldsymbol{D}} \dot{\tilde{\boldsymbol{x}}}_2 + \frac{1}{2} \tilde{\boldsymbol{x}}_2^{\mathrm{T}} \dot{\bar{\boldsymbol{D}}} \tilde{\boldsymbol{x}}_2 - \boldsymbol{s}_2^{\mathrm{T}} \varepsilon \boldsymbol{s}_2 + \boldsymbol{s}_2^{\mathrm{T}} (w - \bar{\boldsymbol{\tau}}_R) \tag{49}$$

where $w = \tilde{\bar{\boldsymbol{D}}}(\ddot{\boldsymbol{q}}_{bld} + L\hat{\boldsymbol{e}}_2) - (\hat{\bar{\boldsymbol{D}}} + \tilde{\bar{\boldsymbol{D}}}) L \tilde{\boldsymbol{x}}_2 + \boldsymbol{\tau}_d + (\bar{\boldsymbol{h}}(\boldsymbol{x}_1, \boldsymbol{x}_2) - \hat{\bar{\boldsymbol{h}}}(\boldsymbol{x}_1, \hat{\boldsymbol{x}}_2))(\dot{\boldsymbol{q}}_{bld} + L\boldsymbol{e}_1)$. According to Property 4, the following equation is derived:

$$\begin{aligned} \|w\| \leq\ & \tilde{\bar{D}}_{max} \left\|\ddot{\boldsymbol{q}}_{bld} + L\hat{\boldsymbol{e}}_2\right\| + \left(\left\|\hat{\bar{\boldsymbol{D}}}\right\|_F + \tilde{\bar{D}}_{max}\right) L \|\tilde{\boldsymbol{x}}_2\| \\ & + \zeta_d + \left(\zeta_{\tilde{\bar{h}}max} (\|\hat{\boldsymbol{x}}_2\| + \|\tilde{\boldsymbol{x}}_2\|) + \zeta_{\hat{\bar{h}}max} \|\tilde{\boldsymbol{x}}_2\|\right) \|\hat{\boldsymbol{s}}_2 + \hat{\boldsymbol{x}}_2\| \end{aligned} \tag{50}$$

where $\hat{\boldsymbol{s}}_2 = \hat{\boldsymbol{e}}_2 + L\boldsymbol{e}_1$, $\dot{\boldsymbol{q}}_{bld} + L\boldsymbol{e}_1 = \hat{\boldsymbol{s}}_2 + \hat{\boldsymbol{x}}_2$.

https://doi.org/10.1017/S0263574716000801 Published online by Cambridge University Press

According to Properties 1-4 and $|\tilde{x}_2^i| < \gamma_1^i$, $\|w\|$ satisfies

$$\begin{aligned}\|w\| &\le \tilde{\bar{D}}_{max}\left\|\ddot{\boldsymbol{q}}_{bld} - L^2\boldsymbol{e}_1\right\| + \zeta_{\bar{\boldsymbol{h}}}\|\hat{\boldsymbol{x}}_2\| + \zeta_{\bar{\boldsymbol{h}}}\|\hat{\boldsymbol{s}}_2\| + \left(\left\|\hat{\bar{\boldsymbol{D}}}\right\|_F + \tilde{\bar{D}}_{max}\right) L\|\boldsymbol{\Lambda}_1\|_F + \zeta_d + L\tilde{\bar{D}}_{max}\|\hat{\boldsymbol{s}}_2\| \\ &\le \zeta_0 + \left(L\tilde{\bar{D}}_{max} + \zeta_{\bar{\boldsymbol{h}}}\right)\|\hat{\boldsymbol{s}}_2\| = \zeta_R(\hat{\boldsymbol{s}}_2, t)\end{aligned} \tag{51}$$

where $\zeta_{\bar{\boldsymbol{h}}} = \zeta_{\tilde{h}max}(\|\hat{\boldsymbol{x}}_2\| + \|\tilde{\boldsymbol{x}}_2\|) + \zeta_{\hat{h}max}\|\tilde{\boldsymbol{x}}_2\| = \zeta_{\tilde{h}max}(\|\hat{\boldsymbol{x}}_2\| + \|\boldsymbol{\Lambda}_1\|_F) + \zeta_{\hat{h}max}\|\boldsymbol{\Lambda}_1\|_F$, $\zeta_0 = \tilde{\bar{D}}_{max}\|\ddot{\boldsymbol{q}}_{bld} - L^2\boldsymbol{e}_1\| + (\|\hat{\bar{\boldsymbol{D}}}\|_F + \tilde{\bar{D}}_{max})L\|\boldsymbol{\Lambda}_1\|_F + \zeta_d + \zeta_{\bar{\boldsymbol{h}}}\|\hat{\boldsymbol{x}}_2\|$.

The following robust control term is proposed:

$$\bar{\boldsymbol{\tau}}_R = \zeta_R(\hat{\boldsymbol{s}}_2, t)\,\mathrm{sgn}(\boldsymbol{s}_2). \tag{52}$$

Then, Eq. (49) becomes

$$\begin{aligned}\dot{V} &= \tilde{\boldsymbol{x}}_2^{\mathrm{T}}\bar{\boldsymbol{D}}\dot{\tilde{\boldsymbol{x}}}_2 + \frac{1}{2}\tilde{\boldsymbol{x}}_2^{\mathrm{T}}\dot{\bar{\boldsymbol{D}}}\tilde{\boldsymbol{x}}_2 - \boldsymbol{s}_2^{\mathrm{T}}\varepsilon\boldsymbol{s}_2 + \boldsymbol{s}_2^{\mathrm{T}}(w - \zeta_R(\hat{\boldsymbol{s}}_2, t)\ \mathrm{sgn}\ (\boldsymbol{s}_2)) \\ &\le -Q_{\min}\|\tilde{\boldsymbol{x}}_2\|^2 + (1 - Q_{\min})\zeta_d^2 - \varepsilon\|\boldsymbol{s}_2\|^2.\end{aligned} \tag{53}$$

When $\boldsymbol{\Lambda}_1, \boldsymbol{\Lambda}_2$ is given appropriately, $\tilde{\boldsymbol{x}}_2$ converges exponentially to a bounded region. Then, applying extended Lyapunov theory[51] and Eq. (53), uniform ultimate boundedness for the tracking errors of the system is guaranteed.

Since $\boldsymbol{x}_2$ is not measured directly, $\boldsymbol{s}_2$ could be obtained by $\hat{\boldsymbol{s}}_2$, that is,

$$\boldsymbol{s}_2 = \hat{\boldsymbol{s}}_2 - \tilde{\boldsymbol{x}}_2 = \hat{\boldsymbol{s}}_2 - \boldsymbol{\Lambda}_1\,\mathrm{sgn}(\boldsymbol{x}_1 - \hat{\boldsymbol{x}}_1).$$

3.2. **Linear observer of the flexible-joint free-flying space manipulator**

Because the pair $(\boldsymbol{A}, \boldsymbol{B})$ of the flexible-joint fast subsystem (31) is completely state controllable, a fast state feedback control can be devised to force its states ζ_2 to zero. Propose the flexible-joint fast controller

$$\boldsymbol{\tau}_{nf} = -\mu\boldsymbol{K}_f\dot{\boldsymbol{\tau}}_l \tag{54}$$

where $\boldsymbol{K}_f \in \mathbf{R}^{2\times 2}$ is a positive-definite diagonal matrix. This sub-controller can stabilize the flexible-joint fast subsystem:

$$\mu^2\boldsymbol{J}_a\ddot{\boldsymbol{\tau}}_l + \mu\boldsymbol{K}_\mu\boldsymbol{K}_f\dot{\boldsymbol{\tau}}_l + \boldsymbol{K}_\mu\boldsymbol{\tau}_l = \boldsymbol{K}_\mu\left(\bar{\boldsymbol{\tau}}_n - \boldsymbol{K}_n^{-1}\boldsymbol{J}_a\ddot{\boldsymbol{q}}_l\right). \tag{55}$$

In order not to measure the space attitude angular velocities and joint velocities, a high gain linear observer is used to robustly estimate the derivatives of output signal of the system.[52]

The tracking error of the system (18) is defined as

$$\boldsymbol{e} = \boldsymbol{q} - \boldsymbol{q}_d$$

where $\boldsymbol{q} = [\,\boldsymbol{q}_{bl}^{\mathrm{T}}\ \boldsymbol{q}_a^{\mathrm{T}}\,]^{\mathrm{T}}$ is the actual output vector, $\boldsymbol{q}_d = [\,\boldsymbol{q}_{bld}^{\mathrm{T}}\ \boldsymbol{q}_{ad}^{\mathrm{T}}\,]^{\mathrm{T}}$ is the desired output vector, $\boldsymbol{q}_{ad} = [\,\theta_{a1d}\ \theta_{a2d}\,]^{\mathrm{T}}$.

Propose a linear observer

$$\begin{aligned}\dot{\hat{\boldsymbol{e}}} &= \boldsymbol{p} + \boldsymbol{L}_d(\boldsymbol{e} - \hat{\boldsymbol{e}}) \\ \dot{\boldsymbol{p}} &= \boldsymbol{L}_p(\boldsymbol{e} - \hat{\boldsymbol{e}})\end{aligned} \tag{56}$$

where $\hat{\boldsymbol{e}} = \hat{\boldsymbol{q}} - \boldsymbol{q}_d$, $\boldsymbol{L}_p = \boldsymbol{L}_p^{\mathrm{T}} > 0$ is the observer proportional gain, $\boldsymbol{L}_d = \boldsymbol{L}_d^{\mathrm{T}} > 0$ is the observer proportional gain, $\hat{\boldsymbol{q}}$ is the estimate of $\boldsymbol{q}$, $\boldsymbol{p}(0) = \boldsymbol{0}$, $\hat{\boldsymbol{e}}(0) = -\boldsymbol{q}_d$.

https://doi.org/10.1017/S0263574716000801 Published online by Cambridge University Press

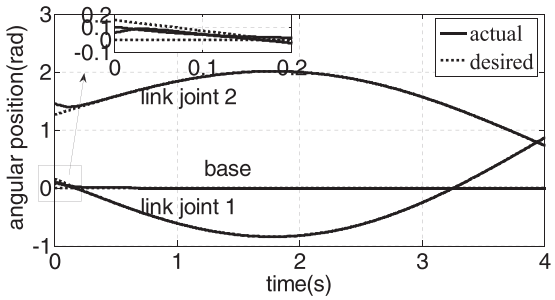


Fig. 3. The comparison between the desired angular displacements and the actual ones of link joints.

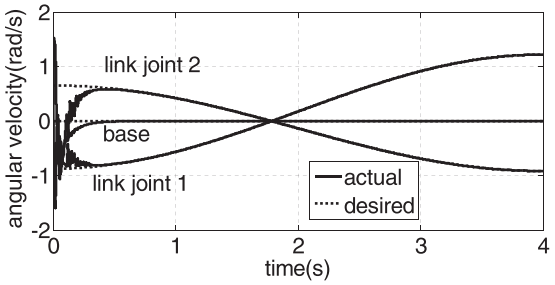


Fig. 4. The comparison between the desired angular velocities and the actual ones of link joints.

According to Eq. (54), the flexible-joint fast control component $\boldsymbol{\tau}_{nf}$ is

$$\boldsymbol{\tau}_{nf} = -\mu \boldsymbol{K}_f \dot{\hat{\boldsymbol{\tau}}}_l \tag{57}$$

where $\dot{\hat{\boldsymbol{\tau}}}_l = -\boldsymbol{K}_{fj}(\dot{\hat{\boldsymbol{q}}}_l - \dot{\hat{\boldsymbol{q}}}_a)$.

4. Simulation Results

To show the performance of the proposed controller, a simulation by the fourth-order Runge–Kutta integration method on Matlab is carried out on a planar space manipulator system shown in Fig. 1. The actual plant parameters of the system are as follows: $l_0 = l_2 = 1.0\,\text{m}$, $l_1 = 2.0\,\text{m}$, $d_1 = 1.0\,\text{m}$, $d_2 = 0.95\,\text{m}$, $m_0 = 200\,\text{kg}$, $m_1 = 8\,\text{kg}$, $m_2 = 16\,\text{kg}$, $I_0 = 100\,\text{kg}\cdot\text{m}^2$, $I_1 = 4.2\,\text{kg}\cdot\text{m}^2$, $I_2 = 42\,\text{kg}\cdot\text{m}^2$, $I_{m1} = I_{m2} = 0.03\,\text{kg}\cdot\text{m}^2$, $k_1 = k_2 = 30\,\text{N}\cdot\text{m/rad}$, $\hat{d}_2 = 0.8\,\text{m}$, $\hat{m}_2 = 6\,\text{kg}$, $\hat{I}_2 = 4.2\,\text{kg}\cdot\text{m}^2$, $\boldsymbol{\tau}_d = 10 \times [\sin(0.25\pi t)\ \cos(0.25\pi t)\ \sin(0.25\pi t)\ -\cos(0.25\pi t)]^{\text{T}}$.

Case 1: The desired trajectories of base's attitude and links' joint angles are chosen as

$$\theta_{0d} = 0, \theta_{1d} = \frac{\pi}{18}t - \frac{4}{3}\sin\left(\frac{\pi}{4}t\right) + 0.05\pi, \theta_{2d} = -\frac{\pi}{24}t + \sin\left(\frac{\pi}{4}t\right) + 0.4\pi,$$

where the unit is in radians. The initial states of the system are chosen as $\theta_0(0) = 0.1\,\text{rad}$, $\theta_1(0) = 0.05\pi - 0.1\,\text{rad}$, $\theta_2(0) = 0.4\pi + 0.2\,\text{rad}$, $\dot{\theta}_0(0) = \dot{\theta}_1(0) = \dot{\theta}_2(0) = 0\,\text{rad/s}$. The time taking in the simulation is 4s. $\boldsymbol{\Lambda}_1 = \text{diag}([10, 10, 10])$, $\boldsymbol{L} = \text{diag}([10, 10, 10])$, $\varepsilon = 50$, $p = 1000$, $\boldsymbol{K}_c = \text{diag}([80, 80])$, $\boldsymbol{K}_n = \text{diag}([81, 81])$, $\boldsymbol{K}_f = \text{diag}([120, 120])$, $\boldsymbol{L}_p = \boldsymbol{L}_d = \text{diag}([262, 262, 262, 262, 262])$.

The controller performances are shown in Figs. 3-6. Figure 3 is the comparison between the desired angular displacements and the actual ones of the base and link joints, whereas Fig. 4 is the comparison between the desired angular velocities and the actual ones of the base and link joints. Figure 5 is the elastic torque observing errors of joints.

https://doi.org/10.1017/S0263574716000801 Published online by Cambridge University Press

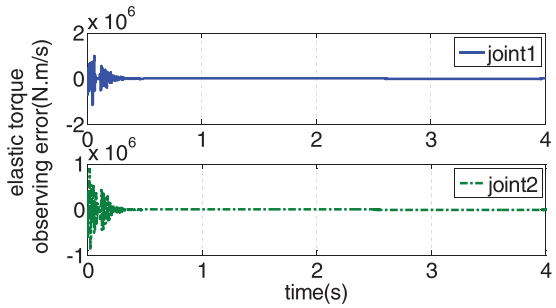


Fig. 5. The elastic torque observing errors of joints.

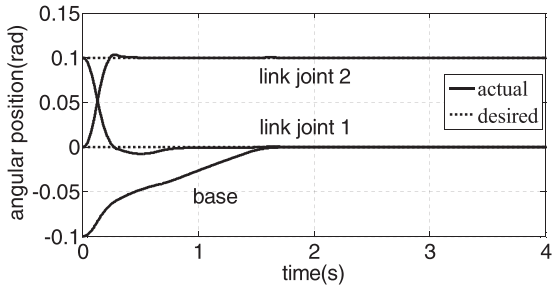


Fig. 6. The comparison between the desired angular displacements and the actual ones of link joints.

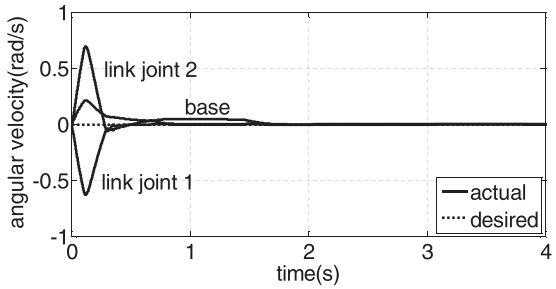


Fig. 7. The comparison between the desired angular velocities and the actual ones of link joints.

It can be seen from Figs. 3 and 4 that good tracking performance is achieved through the application of the proposed observer-based controller. Figure 5 shows that the elastic torque observing errors of joints converge to zero soon.

Case 2: The desired trajectories links' joint angles are chosen as $\theta_{0d} = 0\,\text{rad}$, $\theta_{1d} = 0\,\text{rad}$, $\theta_{2d} = 0.1\,\text{rad}$. The initial states of the system are chosen as $\theta_0(0) = -0.1\,\text{rad}$, $\theta_1(0) = 0.1\,\text{rad}$, $\theta_2(0) = 0\,\text{rad}$. The time taking in the simulation is 4s. $\boldsymbol{\Lambda}_1 = diag([12, 12, 12])$, $\boldsymbol{L} = \text{diag}([12, 12, 12])$, $\varepsilon = 50$, $p = 1000$, $\boldsymbol{K}_c = \text{diag}([80, 80])$, $\boldsymbol{K}_n = \text{diag}([81, 81])$, $\boldsymbol{K}_f = \text{diag}([120, 120])$, $\boldsymbol{L}_p = \boldsymbol{L}_d = \text{diag}([262, 262, 262, 262, 262])$.

The controller performances are shown in Figs. 6-8. Figure 6 is the comparison between the desired angular displacements and the actual ones of the base and link joints, whereas Fig. 7 is the comparison between the desired angular velocities and the actual ones of the base and link joints. Figure 8 is the elastic torque observing errors of joints.

It can be seen from Figs. 6 and 7 that good tracking performance is achieved through the application of the proposed observer-based controller. Figure 8 shows that the elastic torque observing errors of joint converge to zero soon.

https://doi.org/10.1017/S0263574716000801 Published online by Cambridge University Press

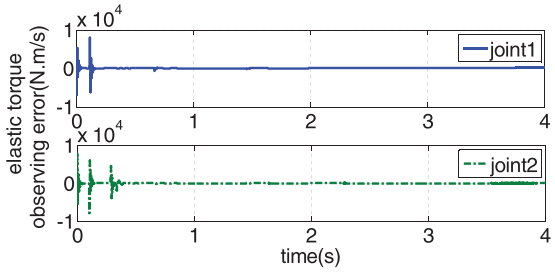


Fig. 8. The elastic torque observing errors of joints.

5. Conclusions

The control problem of a flexible-joint free-flying space robot system with unknown payload parameters and bounded disturbances was discussed in this paper. The dynamic model of the system was derived from the Lagrange equations and momentum conservation law. A flexibility compensator was proposed to make the equivalent joint stiffness large enough to make traditional singular perturbation approach applicable. Then, based on singular perturbation theory, the system was decomposed into two subsystems, a slow subsystem and a fast subsystem. The fast subsystem represents the flexible part, whereas the slow subsystem represents the rigid part. A composite controller that consisted of a slow control component and a fast control component was proposed. A dynamic sliding observer-based robust control algorithm was applied to control the slow subsystem with unknown payload parameters and bounded disturbances. The fast control was designed with the estimated velocity by linear observer to stabilize the fast subsystem around the equilibrium trajectory set up by the slow subsystem under the effect of the slow control. The results of numerical simulations verified the feasibility and efficiency of the proposed control scheme.

The controller proposed does not require measuring the linear position, the linear velocity and the linear acceleration of the spacecraft. In the meantime, the spacecraft attitude angular velocity, link angular and actuator angular velocities need not be measured too.

Acknowledgement

This work was supported by the National Natural Science Foundation of China (No. 11372073), Fujian Provincial Industrial Robot Basic Components' Technology Research Platform (No.2014H21010011) and the Natural Science Foundation of Fujian Province (No. 2016J01228).

Supplementary Material

To view supplementary material for this article, please visit https://doi.10.1017/S0263574716000801.

References

1. R. Boumans and C. Heemskerk, "The European robotic arm for the international space station," *Robot. Auton. Syst.* **23**(1), 17–27 (1998).
2. M. Garneau, "Space in the Service of Society: A Canadian Case Study," *Proceedings of 2nd International Conference on Recent Advances in Space Technologies*, Istanbul, Turkey (2005) pp. 1–6
3. M. Nohmi, "Development of Space Tethered Autonomous Robotic Satellite," *Proceedings of 3rd International Conference on Recent Advances in Space Technologies*, Istanbul, Turkey (2007) pp. 462–467
4. L. B. Holcomb and M. D. Montemerlo, "NASA automation and robotics technology program," *IEEE Aerosp. Electron. Syst. Mag.* **2**(4), 19–26 (2009).
5. K. Yoshida, "Achievements in space robotics[J]," *IEEE Robot. Autom. Mag.* **16**(4), 20–28 (2009).
6. M. W. Walker and L.-B. Wee, "Adaptive control of space-based robot manipulators," *IEEE Trans. Robot. Autom.* **7**(6), 828–835 (1991).
7. Y.-L. Gu and Y. Xu, "A normal form augmentation approach to adaptive control of space robot systems," *Dyn. Control* **5**(3), 275–294 (1995).
8. L. Chen, "Adaptive and Robust Composite Control of Coordinated Motion of Space Robot System with Prismatic Joint," *Proceedings of the 4th World Congress on intelligent Control and Automation*, Shanghai, P. R. China (2002) pp. 1255–1259.

https://doi.org/10.1017/S0263574716000801 Published online by Cambridge University Press

9. L. Chen, "Adaptive Control of Dual-Arm Space Robot System in Joint Space," *Proceedings of the 2006 IEEE/RSJ International Conference on Intelligent Robots and Systems*, Beijing, P. R. China (2006) pp. 5096–5099.
10. Y. S. Guo and L. Chen, "Robust Control of Dual-Arm Space Robot System with Two Objects in Joint Space," *Proceedings of the 2006 IEEE/RSJ International Conference on Intelligent Robots and Systems*, Beijing, China (Oct. 9–15, 2006) pp. 5091–5095.
11. Z. Y. Chen and L. Chen, "Robust Adaptive Composite Control of Space-Based Robot System with Uncertain Parameters and External Disturbances," *Proceedings of the 2009 International Conference on Intelligent Robots and Systems*, St. Louis, MO (Oct. 10–15, 2009) pp. 2353–2358.
12. W. J. Book, "Structural flexibility of motion systems in the space environment," *IEEE Trans. Robot. Autom.* **9**(5), 524–530 (1993).
13. K. Senda and Y. Murotsu, "Methodology for control of a space robot with flexible links," *IEEE Proc. Control Theory Appl.* **47**(6), 562–568 (2000).
14. M. Yoshisada, T. S. Showzow, S. Kei and H. Masato, "Trajectory control of flexible manipulators on a free-flying space robot," *IEEE Control Syst.* **12**(3), 51–57 (1992).
15. A. Green and J. Z. Sasiadek, "Adaptive control of a flexible robot using fuzzy logic," *J. Guid. Control Dyn.* **28**(1), 36–42 (2005).
16. M. Romano, B. N. Agrawal and F. Bernelli-Zazerra, "Experiments on command shaping control of a manipulator with flexible links," *J. Guid. Control Dyn.* **25**(2), 232–239 (2002).
17. Z. H. B. Hong and L. Chen, "Hybrid Control Scheme of Coordinated Motion and Active Vibration Suppression for Free-Floating Space Flexible Manipulator with Parameter Uncertainty," *Proceedings of the ASME 2009 International Design Engineering Technical Conference & Computers and Information in Engineering Conference*, San Diego, CA, USA (Aug. 30–Sep. 2, 2009).
18. J. Carusone, K. S. Buchan and G. M. T. D'Eleuterio, "Experiments in end-effector tracking control for structurally flexible space manipulators," *IEEE Trans. Robot. Autom.* **9**(5), 553–560 (1993).
19. C. J. Damaren, "Modal properties and control system design for two-link flexible manipulators," *Int. J. Robot. Res.* **17**(6), 667–678 (1998).
20. X. Y. Yu and L. Chen, "Singular perturbation adaptive control and vibration suppression of free-flying flexible space manipulators," *Proc. I MechE: Part C: J. Mech. Eng. Sci.* **229**(11), 1989–1997 (2015).
21. C. H. Toglia, M. Sabatini, P. Gasbarri et al., "Optimal target grasping of a flexible space manipulator for a class of objectives," *Acta Astronaut.* **68**, 1031–1041 (2011).
22. M. Sabatini, P. Gasbarri, R. Monti etal., "Vibration control of a flexible space manipulator during on orbit operations," *Acta Astronaut.* **73**, 109–121 (2012).
23. M. Sabatini, P. Gasbarri and G. B. Palmerini, "Delay compensation for controlling flexible space multibodies: Dynamic modeling and experiments," *Control Eng. Practice* **45**, 147–162 (2015).
24. L. M. Sweet and M. C. Good, "Re-Definition of the Robot Motion Control Problem: Effects of Plant Dynamics, Drive System Constraints, and User Requirements," *Proceedings of 23rd IEEE Conference on Decision and Control, Institute of Electrical and Electronics Engineers*, Piscataway, NJ (Dec. 1984) pp. 724–732.
25. P. T. L. M. VanWoerkoma and A. K. Misrab, "Robotic manipulators in space: A dynamics and control perspective," *Acta Astronaut.* **38**(4–8), 411–421 (1996).
26. Y. F. Chen, J. Jin and X. Y. Wu, "Analysis of Dynamical Behavior of a Planetary Gear Train," **In:** *Intelligent Robotics and Applications*, Lecture Notes in Computer Science, vol. 5314 (Springer, Berlin, 2008) pp. 46–53.
27. D. Reintsema, K. Landzettel and G. Hirzinger, "DLR's Advanced Telerobotic Concepts and Experiments for On-Orbit Servicing," **In:** *Advances in Telerobotics* (M. Ferre et al., eds.) (Springer-Verlag, Berlin, 2007) pp. 323–345.
28. M. W. Spong, K. Khorasani and P. V. Kokotovic, "An integral manifold approach to the feedback control of flexible joint robots," *IEEE J. Robot. Autom.* **3**(4), 291–300 (1987).
29. P. Sicard and J. T. Wen, "Application of a Passivity Based Control Methodology for Flexible Joint Robots to a Simplified Space Shuttle RMS," *Proceedings of the 1992 American Control Conference*, Chicago, IL, USA (1992) pp. 1690–1694.
30. Y. R. Hu and G. Vukovich, "Modeling and Control of Free-Flying Flexible Joint Coordinated Robots," *Proceedings of International Conference on Advanced Robotics ICAR* (1997) pp. 1013–1020.
31. S. Ulrich and J. Z. Sasiadek, "Extended Kalman Filtering for Flexible Joint Space Robot Control," *Proceedings of the 2011 American Control Conference* (2011) pp. 1021–1026.
32. X. D. Zhang, Q. X. Jia, H. X. Sun and M. Chu, "The research of space robot flexible joint trajectory control (in Chinese)," *J. Astronaut.* **29**(6), 1865–1870 (2008).
33. B. Pan, J. Sun and D. Y. Yu, "Modeling, control and simulation of space manipulators with flexible joints (in Chinese)," *J. Syst. Simul.* **22**(8), 1826–1831 (2010).
34. L. M. Xie and L. Chen, "Singular Perturbation and Fuzzy Variable Structure Sliding Mode Control of Space Robot System with Flexible Joint in Inertial Space," *Proceedings of 62nd International Astronautical Congress*, Cape Town, South Africa (2011) pp. 5124–5127.
35. Z. Y. Chen and L. Chen, "Robust Neural Network Control of Space Robot System with Flexible Joints," *Proceedings of 63rd International Astronautical Congress*, Naples, Italy (2012) pp. 6762–6767.
36. S. Ulrich, J. Z. Sasiadek and I. Barkana, "Modeling and direct adaptive control of a flexible-joint manipulator," *J. Guid. Control Dyn.* **35**(1), 25–39 (2012).

https://doi.org/10.1017/S0263574716000801 Published online by Cambridge University Press

37. T. Zou, F. L. Ni and CH. Q. Guo *et al.*, "Parameter Identification and Controller Design for Flexible Joint of Chinese Space Manipulator," *Proceedings of the 2014 IEEE International Conference on Robotics and Biomimetics*, Bali, Indonesia (2014) pp. 142–147.
38. X. Y. Yu and L. Chen, "Modeling and observer-based augmented adaptive control of flexible-joint free-floating space manipulators," *Acta Astronaut.* **108**, 146–155 (2015).
39. F. Aghili, "Coordination Control of a Free-Flying Manipulator and its Base Attitude to Capture and Detumble a Noncooperative Satellite," *Proceedings of the 2009 IEEE/RSJ International Conference on Intelligent Robots and Systems*, St. Louis, USA (2009) pp. 2365–2372
40. V. Rutkovsky, V. Sukhanov and V. Glumov, "Free-Flying Manipulation Robot using for in-Orbit Assembly of Large Space Structures," *Proceedings of 5th International Conference on Recent Advances in Space Technologies*, Istanbul, Turkey (2011) pp. 808–813.
41. M. W. Spong, "Modeling and control of elastic joint robots," *J. Dyn. Syst. Meas. and Control* **109**(4), 310–319 (1987).
42. P. Kokotovic, H. K. Khalil and J. O'Reilly, *Singular Perturbation Methods in Control Analysis and Design* (Academic Press, New York, USA, 1986).
43. F. Ghorbel, J. Y. Hung and M. W. Spong, "Adaptive control of flexible-joint manipulators," *IEEE Control Syst. Mag.* **13**(1), 9–13 (1989).
44. Y. C. Liu, M. H. Jin and H. Liu, "Singular perturbation control for flexible-joint manipulator based on flexibility compensation (in Chinese)," *Robot* **30**(5), 460–466 (2008).
45. B. Siciliano, L. Sciavicco, L. Villani and G. Oriolo *Robotics Modelling, Planning and Control* (Springer, London, England, 2009) pp. 257–263.
46. J. E. Slotine and W. Li, "On the adaptive control of robot manipulators," *Int. J. Robot. Res.* **6**(3), 49–59 (1987).
47. R. Ortega and M. W. Spong, "Adaptive Motion Control of Rigid Robots: A Tutorial," *Proceedings of the 27th Conference on Decision and Control*, Austin, TX (1988) pp. 1575–1584.
48. M. A. Arteaga and R. Kelly, "Robot control without velocity measurements: New theory and experimental results," *IEEE Trans. Robot. Autom.* **20**(2), 297–308 (2004).
49. S. Nicosia and P. Tomei, "Robot control by using only joint position measurements," *IEEE Trans. Autom. Control* **35**(9), 1058–1061 (1990).
50. C. C. Wit De and J. J. E. Slotine, "Sliding observers for robot manipulators," *Automatica* **27**(5), 859–864 (1991).
51. F. L. Lewis, C. T. Abdallah and D. M. Dawson, Control of Robot Manipulators (MacMillan, New York, 1993).
52. J. Y. Lee, T. J. Ha, J. S. Yeon, S. H. Lee and J. H. Park "Robust Nonlinear Observer for Flexible Joint Robot Manipulators with only Motor Position Measurement," *Proceedings of the 2007 International Conference on Control, Automation and Systems*, Seoul, South Korea (2007) pp. 56–61.

Appendix: $\mathbf{D}(\mathbf{q}_{bl})$, $\mathbf{J}_a$ and $\mathbf{h}(\mathbf{q}_{bl}, \dot{\mathbf{q}}_{bl})$ in dynamic equation

$$
\begin{aligned}
\boldsymbol{D}(1,1) &= 2\left(B_1 + B_2 + B_3 + B_4\cos(\theta_1) + B_5\cos(\theta_1+\theta_2) + B_6\cos(\theta_2)\right)\\
\boldsymbol{D}(1,2) &= 2\left(B_2 + B_3 + B_6\cos(\theta_2)\right) + B_4\cos(\theta_1) + B_5\cos(\theta_1+\theta_2)\\
\boldsymbol{D}(1,3) &= 2B_3 + B_5\cos(\theta_1+\theta_2) + B_6\cos(\theta_2)\\
\boldsymbol{D}(2,1) &= \boldsymbol{D}(1,2)\\
\boldsymbol{D}(2,2) &= 2\left(B_2 + B_3 + B_6\cos(\theta_2)\right)\\
\boldsymbol{D}(2,3) &= 2B_3 + B_6\cos(\theta_2)\\
\boldsymbol{D}(3,1) &= \boldsymbol{D}(1,3)\\
\boldsymbol{D}(3,2) &= \boldsymbol{D}(2,3)\\
\boldsymbol{D}(3,3) &= 2B_3\\
\boldsymbol{h}(1,1) &= -B_4\dot{\theta}_1\sin(\theta_1) - B_5\left(\dot{\theta}_1+\dot{\theta}_2\right)\sin(\theta_1+\theta_2) - B_6\dot{\theta}_2\sin(\theta_2)\\
\boldsymbol{h}(1,2) &= -B_4\left(\dot{\theta}_0+\dot{\theta}_1\right)\sin(\theta_1) - B_5\left(\dot{\theta}_0+\dot{\theta}_1+\dot{\theta}_2\right)\sin(\theta_1+\theta_2) - B_6\dot{\theta}_2\sin(\theta_2)\\
\boldsymbol{h}(1,3) &= -B_5\left(\dot{\theta}_0+\dot{\theta}_1+\dot{\theta}_2\right)\sin(\theta_1+\theta_2) - B_6\left(\dot{\theta}_0+\dot{\theta}_1+\dot{\theta}_2\right)\sin(\theta_2)\\
\boldsymbol{h}(2,1) &= B_4\dot{\theta}_0\sin(\theta_1) + B_5\dot{\theta}_0\sin(\theta_1+\theta_2) - B_6\dot{\theta}_2\sin(\theta_2)
\end{aligned}
$$

https://doi.org/10.1017/S0263574716000801 Published online by Cambridge University Press

$$\begin{aligned}
\boldsymbol{h}(2,2) &= -B_6\dot{\theta}_2 \sin(\theta_2)\\
\boldsymbol{h}(2,3) &= -B_6\left(\dot{\theta}_0+\dot{\theta}_1+\dot{\theta}_2\right)\sin(\theta_2)\\
\boldsymbol{h}(3,1) &= B_5\dot{\theta}_0\sin(\theta_1+\theta_2)+B_6\left(\dot{\theta}_0+\dot{\theta}_1\right)\sin(\theta_2)\\
\boldsymbol{h}(3,2) &= B_6\left(\dot{\theta}_0+\dot{\theta}_1\right)\sin(\theta_2)\\
\boldsymbol{h}(3,3) &= 0\\
\boldsymbol{J}_a(1,1) &= 2B_7\\
\boldsymbol{J}_a(1,2) &= 0\\
\boldsymbol{J}_a(2,1) &= 0\\
\boldsymbol{J}_a(2,2) &= 2B_8
\end{aligned}$$

where

$$\begin{aligned}
B_1 &= \frac{1}{2}\left(I_0+m_0N_0^2+m_1\left(N_0+l_0\right)^2+m_2\left(N_0+l_0\right)^2\right),\\
B_2 &= \frac{1}{2}\left(I_1+m_0N_1^2+m_1\left(N_1+d_1\right)^2+m_2\left(N_1+l_1\right)^2\right),\\
B_3 &= \frac{1}{2}\left(I_2+m_0N_2^2+m_1N_2^2+m_2\left(N_2+d_2\right)^2\right),\\
B_4 &= m_0N_0N_1+m_1\left(N_0+l_0\right)\left(N_1+d_1\right)+m_2\left(N_0+l_0\right)\left(N_1+l_1\right),\\
B_5 &= m_0N_0N_2+m_1\left(N_0+l_0\right)N_2+m_2\left(N_0+l_0\right)\left(N_2+d_2\right),\\
B_6 &= m_0N_1N_2+m_1\left(N_1+d_1\right)N_2+m_2\left(N_1+l_1\right)\left(N_2+d_2\right),\\
B_7 &= \frac{I_{a1}}{2},\ B_8=\frac{I_{a2}}{2},\ N_0=-\frac{(m_1+m_2)}{M}l_0,\\
N_1 &= -\frac{(m_1d_1+m_2l_1)}{M},\ N_2=-\frac{m_2d_2}{M},\ M=m_0+m_1+m_2.
\end{aligned}$$

https://doi.org/10.1017/S0263574716000801 Published online by Cambridge University Press